Analyses of a composite functionally graded material beam with a new transverse shear deformation function

Hamza Guenfoud [1]✉, Hassina Ziou[2], Mohamed Himeur[1], Mohamed Guenfoud[1]

1 LGCH Laboratory, 8 MAY 1945 University of Guelma, Guelma, Algeria

2 Mohamed Khider University, Biskra, Algeria

Received 12 June 2016
Revised 06 November 2016
Accepted 19 November 2016
Published online: 22 December 2016

Keywords
Functionally Graded Material
Power-law
Finite Element Method
Timoshenko's beam
Shear function

Abstract: In the present paper, we offer a higher-order shear deformation theory for bending of functionally graded beam. A new polynomial shear function is used which satisfies the stress-free boundary conditions (exact boundary conditions on the stress) at both, top and bottom surfaces of the beam. Hence, the shear correction factor is not necessary. Additionally, the present theory has strong similarities with Timoshenko beam theory in some concepts such as equations of movement, boundary conditions and stress resultant expressions. The governing equations and boundary conditions are derived from the principle of minimum potential energy. Functionally graded material FGM beams have a smooth variation of material properties due to continuous (unbroken) change in micro structural details. The variation of material properties is along the beam thickness and assumed to follow a power-law of the volume fraction of the constituents. Finite element numerical solutions obtained with the new polynomial shear function are presented and the obtained results are evaluated versus the existing solutions to verify the validity of the present theory. At last, the influences of power law indicator and the new shear deformation polynomial function on the bending of functionally graded beams are explored.

1. Introduction

The concept of FGM was developed by Japanese material scientists in 1984 for super heat-resistant materials to be used in space planes. Functionally Graded Materials (FGMs) are microscopically inhomogeneous composites that are frequently made from a mixture of metals and ceramics. They are a class of composites that have continuous variation of material properties from the top and the bottom surfaces, of a beam structure for example, and thus eliminate the stress concentration at the interface of the layers found in laminated composites. The combination of different materials with specific physical properties permits an adapted material design that extends the structural design space by implementing a multi-functional response with a minimal weight increase.

Figure 1 presents a FGM beam structure in which the material changes gradually from full metallic at the bottom to full ceramic at the top. The metallic area is used to withstand the mechanical loads, while the ceramic one acts as thermal protection. Owed to growing of FGM applications in engineering structures, various beam theories have been developed to predict the response of functionally graded beams. The first one is the Classical Beam Theory (CBT) recognized as Euler-Bernoulli Beam Theory (EBBT) (Euler 1744). It is the simplest one and is applicable to slight beams only. For moderately thick beams, the CBT underestimates deflection and shear stress due to ignoring the transverse shear deformation effect (Yang 2008, Simsek 2009 and Alshorbagy 2011); this is the reason why it is not applicable for thick beams. The second beam theory is the First-order Shear Deformation Beam Theory (FSDBT). It is recognized as Timoshenko Beam Theory (TBT) (Timoshenko 1921, 1922). It has been proposed to overcome the limitations of the CBT by accounting the transverse shear deformation effect. Since the FSDBT violates the zero shear stress conditions on the both, top and bottom surfaces of the beam. The reason why a shear correction factor is necessary to account for the divergence between the real stress state and the assumed constant stress state (Chakraborty et al. 2003, Li 2008, Sina 2009 and Wei 2012).

To keep away from the use of the shear correction factor and to have a better prediction of beam response; higher-order shear deformation theories (HSDT) have been developed and proposed by many authors; liking the third-order theory of Reddy (TTR) (Reddy 1984, Wang 2000 and Yesilce 2009, 2010, 2011), the hyperbolic theory of Soldatos (1992), the sinusoidal theory of Touratier (1991), the exponential theory of Karama et al. (2003, 2009), and the unified formulation of Carrera (2003) and Carrera et al. (2011).

Aydogdu (2006 & 2009) presented a study in which he compared the different theories of higher order (Parabolic Shear Deformation Theory PSDT, Trigonometric Shear Deformation Theory TSDPT and Exponential Shear Deformation ESDPT) with

✉ Corresponding author. E-mail address: gue2905m@yahoo.fr

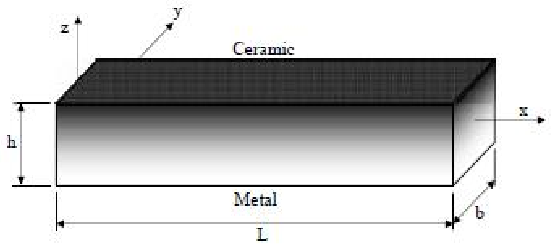

Fig. 1. An example of FGM beam Structure

the elasticity theory of three-dimensional. The author has shown that the transverse displacement and stresses are better predicted by ESDPT compared to other theories.

Generally, in order to increase the accuracy of the results, an increase in the degree of the polynomial of the kinematic equation may be an alternative.

$$U_i(M,t) = U_i(M_0,t) + z w_i^{(1)}(M_0,t) + z^2 w_i^{(2)}(M_0,t) + z^3 w_i^{(3)}(M_0,t) + \cdots, \quad (1)$$

where, z is the normal coordinate.

This technique is not adopted by researchers because of its high cost in terms of calculation. In this context, several simplifications have been proposed to reduce the number of displacement parameters. One of these simplifications is introduced to shorten the last terms of the Taylor series of the "shear function". The form of the proposed movement through the thickness is as follows:

$$u(x,z) = u_0(x) - z\frac{\partial w_0}{\partial x}(x) + f(z)\theta_x(x) \quad (2)$$

$$w(x,z) = w_0(x) \quad (3)$$

$f(z)$ can be considered as the shearing function to determine the distribution of strain and transverse shear stress through the thickness. According to this function f(z), we can distinguish some models of important higher order in the literature that are described in Table.1.

Higher-order shear deformation theories can be developed based on the assumption of a higher-order variation of axial displacement through the thickness of the beam (Aydogdu and Taskin 2007, Kadoli et al. 2008, Simsek 2009, Ben-Oumrane 2009, Li 2010, Simsek 2010 and Wattanasakulpong 2011) or both axial and transverse displacements through the depth of the beam (i.e. via the use of a unified formulation) (Giunta et al. 2010a, 2010b and 2011). In the present paper, we attribute a higher-order shear deformation beam theory for FGM bending beams. This later is based upon a new polynomial shear function that satisfies the zero traction boundary conditions on the top and bottom surfaces of the beam, thus a shear correction factor is not necessary. In addition, the present theory has burly similarities with the Beam Theory CBT in a many expressions such as equations of motion, boundary conditions, and stress resultant expressions.

Material properties of FG beams are supposed to vary according to a power law distribution of the volume fraction of the constituents. Equations of motion and boundary conditions are derived from the principle of minimum potential energy. Numerical examples are presented to display the validity and accuracy of the present shear deformation theory and to show the effects of power law index and shear deformation on the bending of FG beams explored. Numerical solutions for bending are obtained for a many beams solicited by different forces.

2. Material properties of FGM beam and the neutral axis

2.1. Effective material properties of metal ceramic functionally graded beams

Figure 2 presents an FGM beam composed of ceramic and metal of length L, width b and thickness h. Material properties vary continuously and non-uniformly in the z direction. Top surface consists of only ceramic and the bottom surface has only metal. In between volume fraction of ceramic V_c and metal V_m are obtained by power law distribution in conjunction with simple law of constituent mixture as follows:

$$V_c = \left(\frac{z}{h} + \frac{1}{2}\right)^p \quad (4)$$

$$V_m = 1 - V_c \quad (5)$$

where, z = distance from neutral axis and p = power law index, the non-negative variable parameter which dictates the material variation profile through the thickness of the beam a positive real number. The value of p=0 represents a pure ceramic beam; if p is infinite the beam is entirely metallic, for p=1 the variation of the combination of metal and ceramic is linear and when the value of p is increased, content of metal in FGM increases.

The variation of the ceramic volume fraction in the thickness direction of the FGM beams as a function of different values of p is illustrated in Fig. 3.

Table 1. Different shear functions

Shear Functions	Authors
$f(z) = \frac{z}{2}\left(\frac{h^2}{4} - \frac{z^2}{3}\right)$	Ambartsumyan 1958
$f(z) = \frac{5z}{4}\left(1 - \frac{4z^2}{3h^2}\right)$	Kaczkowski 1968, Panc 1975 and Reissner 1975
$f(z) = z\left(1 - \frac{4z^2}{3h^2}\right)$	Levinson 1980, Murthy 1981 and Reddy 1984
$f(z) = \frac{h}{\Pi}sin\left(\frac{\Pi z}{h}\right)$	Levy 1877, Stein 1986 and Touratier 1991
$f(z) = hsin\left(\frac{z}{h}\right) - zcosh\left(\frac{1}{2}\right)$	Soldatos 1992
$f(z) = ze^{-2(z/h)^2}$	Karama et al. 2003, 2009
$f(z) = sin(\Pi z/h)$	Ferreira et al. 2005
$f(z) = z\alpha^{-2(z/h)^2/\ln\alpha}$, $\alpha > 0$	Aydogdu 2009
$f(z) = z\alpha^{-2(z/h)^2}$	Mantari et al. 2011
$f(z) = tan(mz)$	Mantari et al. 2012a
$f(z) = sin(\Pi z/h)e^{m\,cos(\Pi z/h)}$	Mantari et al. 2012b
$f(z) = sin\left(\frac{z}{h}\right)e^{m\,cosh(z/h)}$	Mantari and Soares 2012
$f(z) = sinh^{-1}\left(\frac{rz}{h}\right) - z\frac{2r}{h\sqrt{r^2+4}}$, $r = 3$	Grover et al. 2013
$f(z) = cot^{-1}\left(\frac{rh}{z}\right) - \frac{4r}{h(4r^2+1)}$, $r = 0.46$	Sahoo and Singh 2013

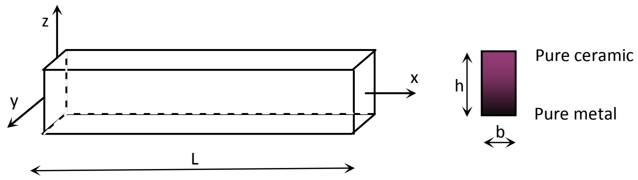

Fig. 2. Geometry of FGM beam and the possible variation of ceramic and metal through thickness

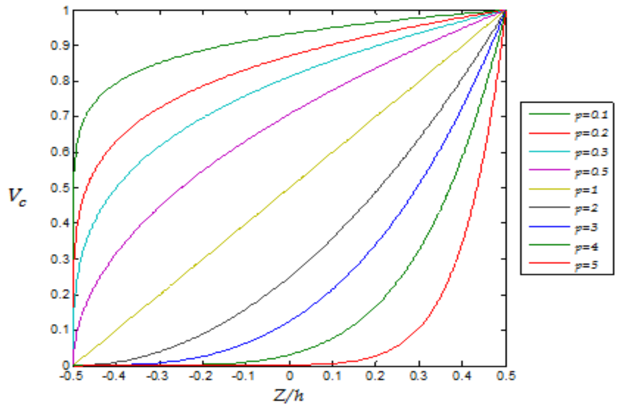

Fig. 3. The variation of the ceramic volume fraction in the thickness direction.

The effective material properties MP_{eff} are evaluated using the relation:

$$MP_{eff} = MP_m V_m(z) + MP_c V_c(z) \; 0 \tag{6}$$

Where, MP_m and MP_c stands for material properties of metals and ceramics respectively. Thus the modulus of elasticity E_{eff}, Poisson's ratio ν_{eff}, and shear modulus G_{eff}, of FGMs can be given by:

$$E_{eff} = (E_c - E_m)\left(\frac{z}{h} + \frac{1}{2}\right)^p + E_m \tag{7-a}$$

$$\nu_{eff} = (\nu_c - \nu_m)\left(\frac{z}{h} + \frac{1}{2}\right)^p + \nu_m \tag{7-b}$$

$$G_{eff} = (G_c - G_m)\left(\frac{z}{h} + \frac{1}{2}\right)^p + G_m \tag{7-c}$$

Using the above relation it is possible to obtain an approaching into the variation of the material properties across the thickness of the beam for different power law indexes. Figures 4 illustrate the variation of Young's modulus, Poisson's ratio and shear modulus of an FGM beam.

It has been confirmed by Delale (1983) and Ziou et al. (2016) with an energetic method that the variation of the Poisson coefficient does not have much influence on the evaluation of deformation. Therefore, we kept the same Poisson coefficient for both materials.

2.2 Position of the neutral axis

Before the resoluteness of a desirable solution, the position of the neutral axis must be known. Visibly, due to varying of material properties of the beam (the Young's modulus precisely), the neutral axis is no longer at the midline, but moved from the midline except for a beam with symmetrical Young's modulus. To determine the position of the neutral axis, we construct a new coordinate system such that the new x axis is positioned at the neutral axis, which will be determined as follow. Subsequently we have:

$$x = x' \qquad z = z' + h_0 \tag{8}$$

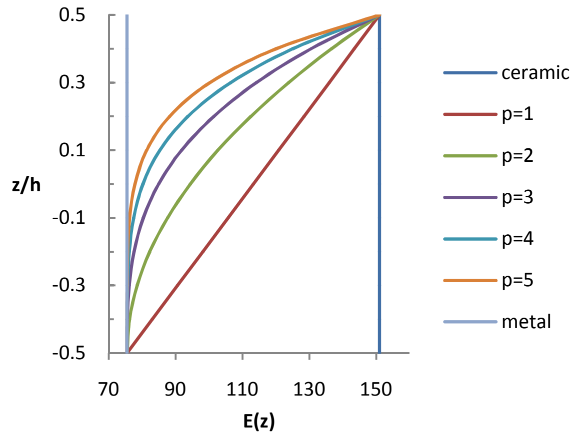

(a) Young's Modulus E (z)

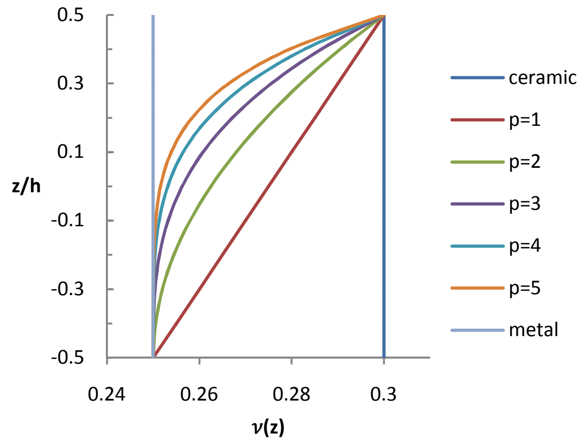

(b) Poisson's ratio v (z)

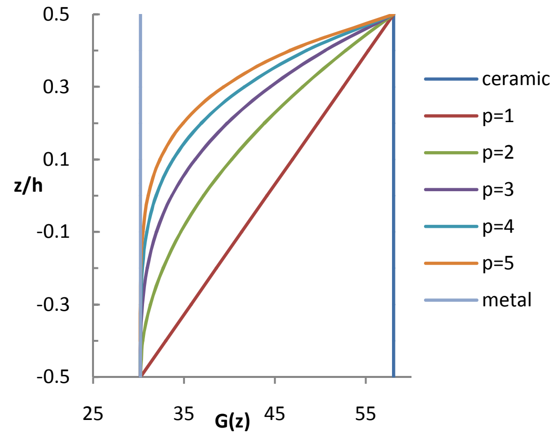

(c) Shear Modulus G (z)

Fig. 4. Variations of Young's modulus, Poisson's ratio and Shear modulus of an FGM beam along the thickness for various power law indexes.

Where, h0 is the distance between the neutral axis and midline of the beam. In this case and similarly to the usual treatment in the Euler-Bernoulli beam theory (EBBT), we can directly write:

$$\varepsilon_{xx} = -z' \frac{d^2w}{dx^2} \text{ and } \sigma_{xx} = E(z')\, \varepsilon_{xx} \tag{9}$$

Where w is the deflection of the FGM beam. The position of the neutral axis can be determined by choosing h0 such that the total axial force at the cross-section becomes zero:

$$\sum F_x = 0 \int_{h_0-\frac{h}{2}}^{\frac{h}{2}-h_0} \sigma_{xx}\ dA = 0 \tag{10}$$

Substituting equation (8) jointly with (9) into (10) result in

$$\int_{-h_0-\frac{h}{2}}^{\frac{h}{2}-h_0} b.\, E(z').\, z'.\frac{d^2w}{dx^2} dz' = 0 \tag{11}$$

With changing the interval of the integral, we obtain:

$$\int_{-\frac{h}{2}}^{\frac{h}{2}} b.\, E(z').\, (z-h_0).\frac{d^2w}{dx^2} dz = 0 \tag{12}$$

Then

$$b.\frac{d^2w}{dx^2}\left(\int_{-\frac{h}{2}}^{\frac{h}{2}} E(z).\, z.\, dz - h_0 \int_{-\frac{h}{2}}^{\frac{h}{2}} E(z).\, dz\right) = 0 \tag{13}$$

The position of the neutral axis becomes

$$h_0 = \frac{\int_{-\frac{h}{2}}^{\frac{h}{2}} E(z).z.dz}{\int_{-\frac{h}{2}}^{\frac{h}{2}} E(z).dz} \tag{14}$$

With

$$\widehat{D}_{aa} = b\int_{-h/2}^{+h/2} E(z)dz = bh\left(E_m + \frac{E_c - E_m}{p+1}\right) \tag{15-a}$$

$$\widehat{D}_{ab} = b\int_{-h/2}^{+h/2} E(z)zdz = \frac{bh^2}{2}(E_c - E_m)\left[\frac{p}{(p+1)(p+2)}\right] \tag{15-b}$$

$$\widehat{D}_{bb} = b\int_{-h/2}^{+h/2} E(z)z^2dz = \frac{bh^2}{12}\left[3(E_c - E_m)\frac{p^2+p+2}{(p+3)(p+2)(p+1)}\right] \tag{15-c}$$

The substitution of the equation (15-a) and (15-b) into equation (14) gives

$$\frac{h_0}{h} = \frac{(E_c - E_m)\frac{p}{(p+2)(2p+2)}}{E_m + \frac{E_c - E_m}{p+1}} \tag{16}$$

The value of p that maximizes the function h0/h is given by:

$$p = \sqrt{2\frac{E_c}{E_m}} \tag{17}$$

3. Kinematics and stress-strain relations

Let us consider a straight beam of length L and axis x linking the gravity centers G of all cross-sections with x-z being a principal plane of inertia. Here, the coordinate axes are chosen such that the x-axis is oriented in the axial direction at the mid-line of the unbent beam, and the positive z-axis is directed upward and perpendicular to the x-axis, as shown in Fig. 5.

The cross-section is formed by an FGM composite material. Hence, in general the beam axis does not coincide with the neutral axis. The loads are vertical forces and bending moments contained in the x-z plane as usual for plane beams. Bending on the plane y-z will not be considered here. Timoshenko hypothesis for the rotation of the normal to hold will be assumed. The axial and vertical displacements of a point A of the beam section are expressed as

$$u(x,z) = u_0(x) - z\frac{\partial w_0}{\partial x}(x) + f(z)\psi_x(x) \tag{18-a}$$

$$w(x,z) = w_0(x) \tag{18-b}$$

Where:

- $f(z)\psi_x(x)$ is the warping function.

- $u(x,z)$ represents the longitudinal displacement of any points at the transverse section.

w_0 is the transverse deflection of the beam along the z-axis,

$u_0(x) = u(x, z=0)$ is the longitudinal displacement at the mid-line of the beam down the x-axis.

$f(z)$ is the new shear function adopted in the present study.

$$f(z) = z\left(\frac{9}{8} - \frac{9z^2}{6h^2}\right) = z\left(\frac{9}{8} - \frac{9}{6}\left(\frac{z}{h}\right)^2\right) = \frac{9}{8}z - \frac{9z^3}{6h^2} \tag{19}$$

$$f'(z) = \left(\frac{9}{8} - \frac{9z^2}{2h^2}\right) \tag{20}$$

$$f''(z) = -\left(\frac{9z}{h^2}\right) \tag{21}$$

For the classical beam theory CBT (Euler-Bernoulli beam theory EBBT): $f(z) = 0$, and for the First-order Shear Deformation Beam Theory FSDBT (Timoshenko beam theory TBT): $f(z) = z$.

Where $\psi_x(x)$ is the shear strain at the mid-line of the beam.

$$\psi_x(x) = \gamma_{xz}(x, z=0) \tag{22}$$

The nonzero components of the strain tensor are:

$$\varepsilon_x(x,z) = \frac{\partial u_0}{\partial x} - z\frac{\partial^2 w}{\partial x^2} + f(z)\frac{\partial \psi_x}{\partial x} \tag{23}$$

$$\gamma_{xz}(x,z) = \frac{\partial f}{\partial z}.\, \psi_x \tag{24}$$

$f'(z)$ is equal zero at both, top and bottom fiber,($z = \pm h\,/\,2$) which implies the nullity of the shear stress at theses fibers. It is clear that $f''(z)$ is equal zero at z=0. Thus implies that the shear stress is maximal at the midline fiber.

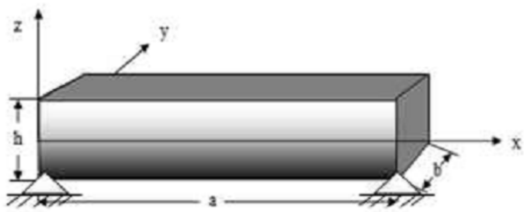

Fig.5. A functionally graded beam element in their axis

Introducing the $f(z)$ function at the equation (18-a), we obtain:

$$u(x,z) = u_0(x) - z\frac{\partial w_0}{\partial x} + \left(\frac{9}{8}z - \frac{9z^3}{6h^2}\right)\psi_x \tag{25-a}$$

$$u(x,z) = u_0(x) - z\left(\frac{\partial w_0}{\partial x} - \frac{9}{8}\psi_x\right) + \frac{9z^3}{6h^2}\psi_x \tag{25-b}$$

The equation (25) has the same form of the equations used per different authors as Levinson (1980), Murthy (1981), Reddy (1984), for higher-order shear deformation theories (HSDT):

$$u(x,z) = u_0(x) + zu_1(x) + z^2u_2(x) + z^3u_3(x) \tag{26}$$

Because the shear stress is zero on the two fibers of the beam ($z = \pm h\,/\,2$). The relation between the shear strain and stress indicate that the shear strain also must vanish. After that, it is clear that $u_2(x)$ must equal zero. So, the equation (26) must be:

$$u(x,z) = u_0(x) + zu_1(x) + z^3u_3(x) \tag{27}$$

Simple to derivate, simple to integrate and simple to program in a finite element code.
In the present analysis and for simplicity, the beam deflection w is assumed independent of the thickness, which is frequent and true enough in classical and higher-order theories for analysis of beams (Savoia 1996).

To develop the final governing equation, initially, taking into account the shear traction-free boundary condition at the beam extreme lines (fibers), shear deformation $\gamma_{xz}(x,z)$ gets the form:

$$\gamma_{xz}(x,z) = \frac{\partial f}{\partial z}.\psi_x = \left(\frac{9}{8} - \frac{9z^2}{6h^2}\right)\psi_x \tag{28}$$

Where ψ_x is shear strain at the mid-line of the beam. It is noted that there are further expressions which would satisfy the necessary boundary conditions.

Equation (19) is, yet, one of the simplest expressions; because; it is a polynomial function characterized by: It is continuous and regular function

At the present, we introduce the rotation angle of cross-section perpendicular to the mid-line as $\theta = \frac{\partial u}{\partial z}$ when $z = 0$, consequently, we have:

$$\psi_x(x) = \theta + \frac{\partial w}{\partial x} \tag{29}$$

So, the normal strain $\varepsilon_x(x,z) = \frac{\partial u}{\partial x}$ can be expressed in terms of the transverse deflection w and the rotation of the section by:

$$\varepsilon_x(x,z) = \frac{\partial u_0}{\partial x} - z\frac{\partial^2 w}{\partial x^2} + \left(\frac{9z}{8} - \frac{9z^3}{2h^2}\right)\frac{\partial \theta}{\partial x} + \left(\frac{9z}{8} - \frac{9z^3}{2h^2}\right)\frac{\partial^2 w}{\partial x^2} \tag{30-a}$$

$$\gamma_{xz}(x,z) = \frac{\partial f}{\partial z}.\psi_x = \left(\frac{9}{8} - \frac{9z^2}{2h^2}\right)\left(\theta + \frac{\partial w}{\partial x}\right) \tag{30-b}$$

It is clear that if $z = 0$ the axial strain is equal to $\varepsilon_x(x,z) = \frac{\partial u_0}{\partial x}$

4. Numerical Results

Let us consider an FGM beam with a rectangular cross-section. The dimensions of the section are: h=0.1m and b=h/100=0.001m. The beam has a length L. Two cases are considered; the span to height ratio L/h is as high as 100 (for the slender beam) and as low as 5 (for deep beam). Young's modulus is graded according to the power law (see equation (7-a)). With Ec=10000 GPa and Em=Ec/10=1000 GPa. The Poisson ratio is equal to 0.25. The beam undergoes a uniform pressure equal one Pa applied at top fiber. The non-dimensional quantities used here are $\frac{E_c}{E_m} = 10$, $\frac{G_c}{G_m} = 10$.

The deflection of the beam is shown in (Fig. 6) and (Fig.7) for various power law exponent, p and for different length-to-thickness (L/h=100, L/h=5 respectively). For FGM beam, transverse deflection increases as power law exponent p is increased. As seen from (Fig .8) and (Fig. 9) the axial stress distribution is linear for full ceramic and also the values of tensile and compressive stresses are equal for isotropic beam (full ceramic).

4.1. Case 1: Thin beam for L/h=100

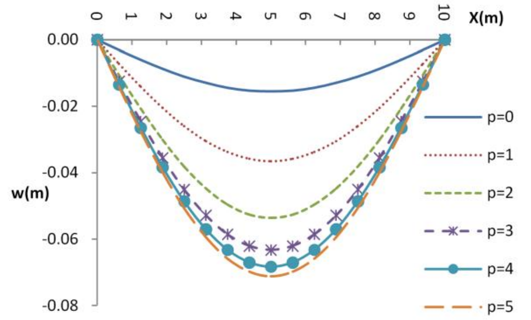

Fig. 6. Variation of transverse deflection w with respect to the power law index p for FGM beam under uniform load (L/h=100).

4.2. Case 2: Thick beam for L/h=5

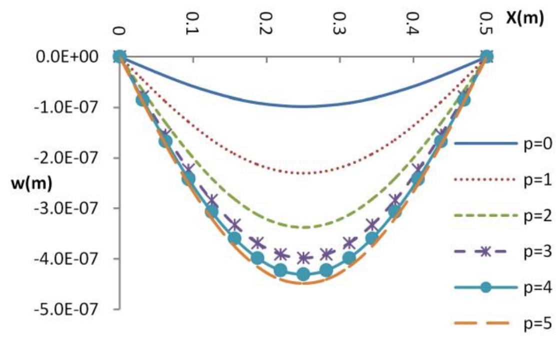

Fig.7. Variation of transverse deflection w with respect to the power law index p for FGM beam under uniform load (L/h=5)

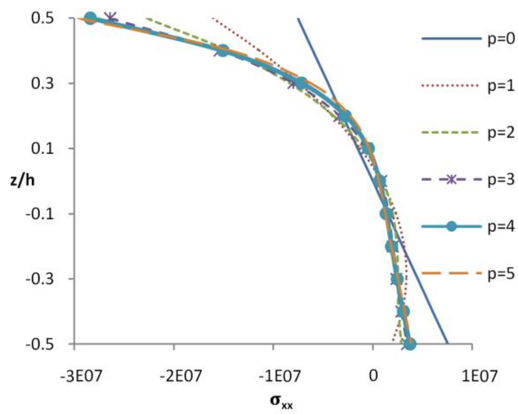

Fig.8. Variation of axial normal stress across the depth of FGM beam under uniform load (L/ h=100).

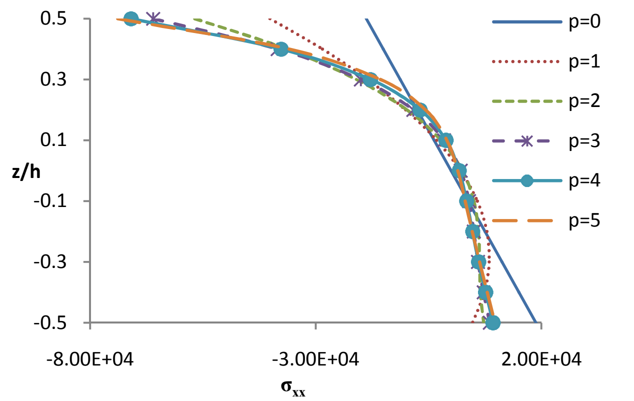

Fig.9. Variation of axial normal stress across the depth of FGM beam under uniform load (L/h=5).

For other values of p, the axial stress distribution is not linear and also the values of compressive stresses are greater than tensile stresses. The value of axial stress is zero at the mid-plane but it is clearly visible that the values of axial stresses are not zero at the mid-plane of the FG beam for the other values of p; it indicates that the neutral plane of the beam moves towards the upper side of the beam for FG beam. This is due to the variation of the modulus of elasticity through the thickness of the FG beam.

Figures 10 and 11 depicts the variation of the shear stress across the thickness of beam for different length-to-thickness (L/h=100, L/h=5 respectively) with different higher order shear deformation theory at x=0. It can be observed that the curves obtained using the new shear deformation beam theory are in good agreement with those given the other beam theories (Kaczkowski 1968 and Levinson 1980) for all values of power law index *p* and span-to-depth ratio L/h.

5. Conclusion

We developed a new higher-order shear-deformation beam theory for bending of functionally graded beams. The developed theory account for higher-order variation of transverse shear strain through the depth of the beam, and satisfy the stress-free boundary conditions on the top and bottom surfaces of the beam. The shear correction factor is not required.

In addition, finite element numerical solutions obtained with the new polynomial shear function are presented. This new function has strong convergence with the other higher order shear-deformation beam theories (Kaczkowski 1968 and Levinson 1980) for various power law exponent p and for different length-to-thickness. In general, all shear deformation beam models give different results, for the case of transverse shear stress. The different transverse shear strain shape functions used in each models can explain it.

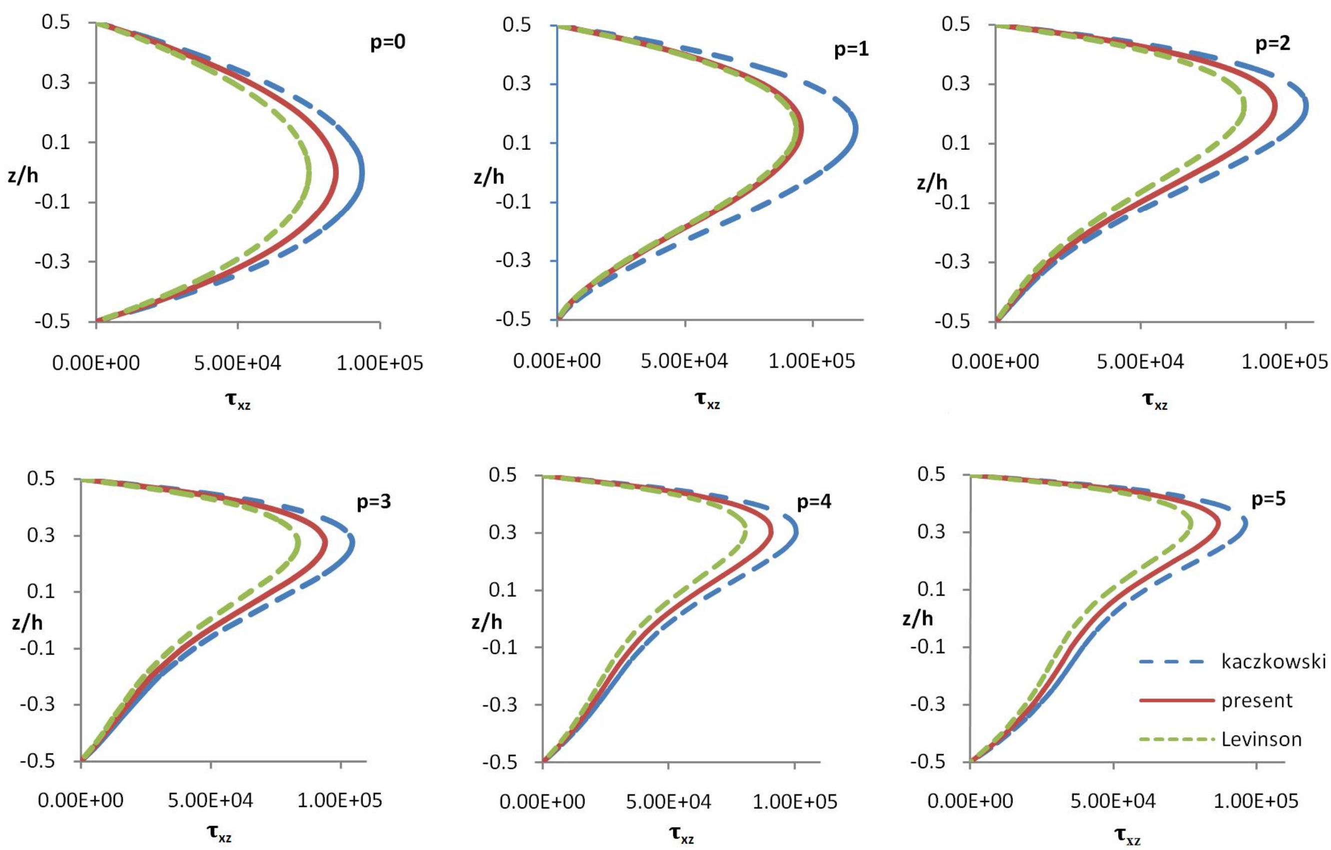

Fig.10. Variation of transverse shear stress across the depth of FGM beam under uniform load for different higher order shear deformation theory at (x=0) (L/h=100).

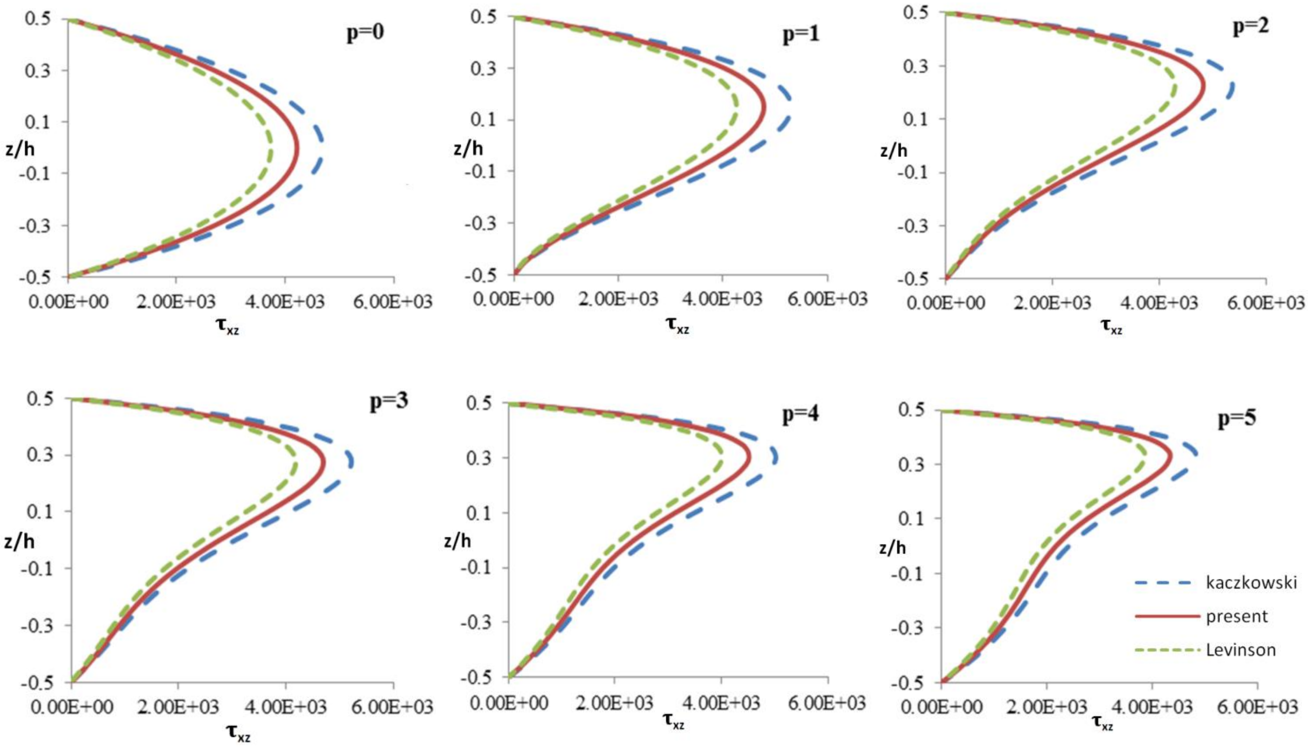

Fig.11. Variation of transverse shear stress across the depth of FGM beam under uniform load for different higher order shear deformation theory at (x=0) (L/h=5).

References

Alshorbagy A.E., M.A. Eltaher, F.F. Mahmoud (2011) Free vibration characteristics of a functionally graded beam by finite element method. Applied Mathematical Modelling 35(1): 412-425.

Ambartsumyan, S.A. (1958) On a general theory of bending theory of anisotropic plates and shallow shells. Investiia Akad. Nauk SSSR. Proceedings of the USSR Academy of Sciences, No. 5, 69-77.

Aydogdu, M. (2006) Comparison of various shear deformation theories for bending, buckling, and vibration of rectangular symmetric cross-ply plate with simply supported edges. Journal of Composite materials 40(23): 2143-2155.

Aydogdu, M. (2009) A new shear deformation theory for laminated composite plates. Composite structures, 89(1): 94-101.

Aydogdu, M., V. Taskin (2007) Free vibration analysis of functionally graded beams with simply supported edges. Materials and Design 28(5): 1651-1656.

Ben-Oumrane, S., T. Abedlouahed, M. Ismail, B.B. Mohamed, M. Mustapha, & A.B. El Abbas (2009) A theoretical analysis of flexional bending of Al/Al 2 O 3 S-FGM thick beams. Computational Materials Science, 44(4): 1344-1350.

Carrera, E. (2003) Theories and finite elements for multilayered plates and shells: a unified compact formulation with numerical assessment and benchmarking. Archives of Computational Methods in Engineering 10(3):215-296.

Carrera, E., G. Giunta, M. Petrolo (2011) Beam Structures: Classical and Advanced Theories. West Sussex, UK, John Wiley & Sons, Ltd.

Chakraborty, A., S. Gopalakrishnan, J.N. Reddy (2003) A new beam finite element for the analysis of functionally graded materials. International Journal of Mechanical Sciences 45(3): 519-539.

Delale, F., F. Erdogan (1983) The crack problem for a nonhomogeneous plane. Journal of Applied Mechanics 50(3): 609-614.

Euler, L. (1744). Methodus inveniendi lineas curvas maximi minimive propietate gaudentes, Additamentum I, De curvis elasticis. Lausanne, Genf: Bousqet & Socios.

Ferreira, A.J.M., C.M.C. Roque, R.M.N. Jorge (2005) Analysis of composite plates by trigonometric shear deformation theory and multiquadrics. Computers & structures 83(27): 2225-2237.

Giunta, G., D. Crisafulli, S. Belouettar, E. Carrera (2011) Hierarchical theories for the free vibration analysis of functionally graded beams. Composite Structures 94(1): 68-74.

Giunta, G., S. Belouettar, E. Carrera (2010a) Analysis of FGM beams by means of classical and advanced theories. Mechanics of Advanced Materials and Structures 17(8): 622-635.

Giunta, G., S. Belouettar, E. Carrera (2010b) Analysis of FGM beams by means of a unified formulation. IOP Conference Series: Materials Science and Engineering 10(1): 012073.

Grover, N., D. Maiti & B. Singh (2013) A new inverse hyperbolic shear deformation theory for static and buckling analysis of laminated composite and sandwich plates. Composite Structures 95: 667-675.

Kaczkowski, Z. (1968) Plates-statistical calculations. Warsaw: Arkady.

Kadoli, R., K. Akhtar & N. Ganesan (2008) Static analysis of functionally graded beams using higher order shear deformation theory. Applied Mathematical Modelling, 32(12), 2509-2525.

Karama, M., K.S. Afaq & S. Mistou (2003) Mechanical behaviour of laminated composite beam by the new multi-layered laminated composite structures model with transverse shear stress continuity. International Journal of Solids and Structures, 40(6): 1525-1546.

Karama, M., K.S. Afaq & S. Mistou (2009) A new theory for laminated composite plates. Proceedings of the Institution of Mechanical Engineers, Part L: Journal of Materials Design and Applications, 223(2): 53-62.

Levinson, M. (1980) An accurate, simple theory of the statics and dynamics of elastic plates. Mechanics Research Communications, 7(6): 343-350.

Levy, M. (1877) Mémoire sur la théorie des plaques élastiques planes. Journal de mathématiques pures et appliquées : 219-306.

Li, X.F. (2008) A unified approach for analyzing static and dynamic behaviors of functionally graded Timoshenko and Euler–Bernoulli beams. Journal of Sound and vibration, 318(4): 1210-1229.

Li, X.F., B.L. Wang & J.C. Han (2010) A higher-order theory for static and dynamic analyses of functionally graded beams. Archive of Applied Mechanics, 80(10): 1197-1212.

Mantari, J. L., A.S. Oktem & C.G Soares (2011) Static and dynamic analysis of laminated composite and sandwich plates and shells by using a new higher-order shear deformation theory. Composite structures, 94(1): 37-49.

Mantari, J.L. & C.G. Soares (2012) Analysis of isotropic and multilayered plates and shells by using a generalized higher-order shear deformation theory. Composite Structures, 94(8): 2640-2656.

Mantari, J.L. A.S. Oktem & , C.G. Soares (2012a) A new higher order shear deformation theory for sandwich and composite laminated plates. Composites Part B: Engineering, 43(3): 1489-1499.

Mantari, J.L., A.S. Oktem & C.G. Soares (2012b) A new trigonometric shear deformation theory for isotropic, laminated composite and sandwich plates. International Journal of Solids and Structures, 49(1): 43-53.

Murthy, M.V.V. (1981) An improved transverse shear deformation theory for laminated anisotropic plates. NASA Technical Paper 1903, 37pp.

Panc, V. (1975) Theories of elastic plates (Vol. 2). Springer Science & Business Media.

Reddy, J.N. (1984) A simple higher-order theory for laminated composite plates. Journal of applied mechanics, 51(4): 745-752.

Reissner, E. (1975) On transverse bending of plates, including the effect of transverse shear deformation. International Journal of Solids and Structures, 11(5): 569-573.

Sahoo, R., & B.N. Singh (2013) A new shear deformation theory for the static analysis of laminated composite and sandwich plates. International Journal of Mechanical Sciences, 75: 324-336.

Savoia, M., & N. Tullini (1996) Beam theory for strongly orthotropic materials. International journal of solids and structures, 33(17): 2459-2484.

Şimşek, M. (2009) Static analysis of a functionally graded beam under a uniformly distributed load by Ritz method. Int J Eng Appl Sci, 1(3): 1-11.

Şimşek, M. (2010) Fundamental frequency analysis of functionally graded beams by using different higher-order beam theories. Nuclear Engineering and Design 240(4): 697-705.

Sina, S.A., Navazi, H.M., & H. Haddadpour (2009) An analytical method for free vibration analysis of functionally graded beams. Materials & Design 30(3): 741-747.

Soldatos, K.P. (1992) A transverse shear deformation theory for homogeneous monoclinic plates. Acta Mechanica 94(3-4): 195-220.

Stein, M. (1986) Nonlinear theory for plates and shells including the effects of transverse shearing. AIAA journal 24(9): 1537-1544.

Timoshenko, S. P. (1921) On the correction for shear of the differential equation for transverse vibrations of prismatic bars. The London, Edinburgh, and Dublin Philosophical Magazine and Journal of Science 41: 744-746.

Timoshenko, S. P. (1922). On the transverse vibrations of bars of uniform cross-section. The London, Edinburgh, and Dublin Philosophical Magazine and Journal of Science 43: 125-131.

Touratier, M. (1991) An efficient standard plate theory. International journal of engineering science 29(8): 901-916.

Wang, C. M., , J.N. Reddy & K.H. Lee (Eds.) (2000) Shear deformable beams and plates: Relationships with classical solutions. Elsevier.

Wattanasakulpong, N., B.G. Prusty & D.W. Kelly (2011) Thermal buckling and elastic vibration of third-order shear deformable functionally graded beams. International Journal of Mechanical Sciences 53(9): 734-743.

Wei, D., Y. Liu & Z. Xiang (2012). An analytical method for free vibration analysis of functionally graded beams with edge cracks. Journal of Sound and Vibration 331(7), 1686-1700.

Yang, J. & Y. Chen (2008) Free vibration and buckling analyses of functionally graded beams with edge cracks. Composite Structures 83(1): 48-60.

Yesilce, Y. & H.H. Catal (2011) Solution of free vibration equations of semi-rigid connected Reddy–Bickford beams resting on elastic soil using the differential transform method. Archive of Applied Mechanics 81(2): 199-213.

Yesilce, Y. & S. Catal (2009) Free vibration of axially loaded Reddy-Bickford beam on elastic soil using the differential transform method. Struct. Eng. Mech 31(4): 453-476.

Yesilce, Y. (2010) Effect of axial force on the free vibration of Reddy-Bickford multi-span beam carrying multiple spring-mass systems. Journal of Vibration and Control 16(1): 11-32.

Ziou, H., H. Guenfoud, & M. Guenfoud (2016) Numerical modelling of a Timoshenko FGM beam using the finite element method. International Journal of Structural Engineering 7(3): 239-261.

Appendix –A-The FGM Beam Element

For an FGM beam with constant section and unloaded, the two equilibrium equations are:

$$\frac{\partial}{\partial x}\left(\frac{\partial w}{\partial x}-\theta_z\right)=0,\ E\frac{\partial^2\theta_z}{\partial x^2}B\int y^2 dz+GAK_z\left(\frac{\partial w}{\partial x}-\theta_z\right)=0 \qquad (A1)$$

A.1. Axial stiffness

The axial stiffness matrix K is:

$$[K_m]=b\int E(z)dz\begin{bmatrix}1/L & -1/L\\ -1/L & 1/L\end{bmatrix} \qquad (A2)$$

A.2. Beam element

The stiffness matrix [K] for the simple beam element is

$$[K]=[K_f]+[K_c]=$$
$$b\int_0^l E(z)z^2 dz\,[B_f]^T[B_f]dx+bK_z\int_0^l G(z)dz[B_c]^T[B_c]dx \qquad (A3)$$

$$[B_f]=\left[\frac{dN_{\theta_z}}{dx}\right],$$
$$[B_c]=\left[\frac{dN_w}{dx}\right]-\left[N_{\theta_z}\right]=\frac{\phi_z}{2L(1+\phi_z)}\begin{bmatrix}-2 & -L & 2 & -L\end{bmatrix}$$

$$K_f=\int E(z)z^2\frac{\partial\theta}{\partial x}\frac{\partial\delta\theta}{\partial x}dv^e$$

A.2.1. Bending stiffness

$$[K_f] = \frac{\widehat{D}_b}{(1+\phi_z)^2}\begin{bmatrix} \frac{12}{L^3} & \frac{6}{L^2} & \frac{-12}{L^3} & \frac{6}{L^2} \\ & \frac{(4+2\phi_z+\phi_z{}^2)}{L} & \frac{-6}{L^2} & \frac{(2-2\phi_z-\phi_z{}^2)}{L} \\ & & \frac{12}{L^3} & \frac{-6}{L^2} \\ & & & \frac{(4+2\phi_z+\phi_z{}^2)}{L} \end{bmatrix} \quad (A4)$$

A.2.2. Shear stiffness

$$K_c = \int G(z)\,K_z\left(\frac{\partial w}{\partial x} - \theta\right)\left(\frac{\partial \delta w}{\partial x} - \delta\theta\right) dv^e$$

$$[K_c] = \frac{\phi_z{}^2\widehat{D}_s}{(1+\phi_z)^2}\begin{bmatrix} \frac{1}{L} & \frac{1}{2} & \frac{-1}{L} & \frac{1}{2} \\ & \frac{L}{4} & \frac{-1}{2} & \frac{L}{4} \\ & & \frac{1}{L} & \frac{-1}{2} \\ & & & \frac{L}{4} \end{bmatrix} \quad (A5)$$

K_f and K_c are elementary matrix calculated by integration over the geometry of an element because their expressions have a polynomial forms :

$$[K] = \frac{\widehat{D}_b}{L^3(1+\phi_z)}\begin{bmatrix} 12 & 6L & -12 & 6L \\ & L^2(4+\phi_z) & -6L & L^2(2-\phi_z) \\ & & 12 & -6L \\ & & & L^2(4+\phi_z) \end{bmatrix} \quad (A6)$$

A.2.3. Coupling axial-bending stiffness

$$K_{cp} = -\int E(z)\frac{\partial \delta u^0}{\partial x}\, z\, \frac{\partial \theta}{\partial x} dv^e$$

The coupling matrix is defined by the equation below:

$$[K_{cp}] = -\widehat{D}_{ab}\begin{bmatrix} 0 & 0 \\ \frac{1}{L} & \frac{-1}{L} \\ 0 & 0 \\ \frac{-1}{L} & \frac{1}{L} \end{bmatrix} \quad (A7)$$

Combining the axial stiffness (bar element), we obtain the stiffness matrix of a general 2-D beam element.

$$[K] = \begin{bmatrix} \frac{EA}{L} & 0 & -\frac{\widehat{D}_{ab}}{L} & \frac{-EA}{L} & 0 & \frac{\widehat{D}_{ab}}{L} \\ & \frac{12\widehat{D}_b}{L^3(1+\phi_z)} & \frac{6\widehat{D}_b}{L^2(1+\phi_z)} & 0 & \frac{-12\widehat{D}_b}{L^3(1+\phi_z)} & \frac{6\widehat{D}_b}{L^2(1+\phi_z)} \\ & & \frac{\widehat{D}_b(4+\phi_z)}{L(1+\phi_z)} & 0 & \frac{-6\widehat{D}_b}{L^2(1+\phi_z)} & \frac{\widehat{D}_b(2-\phi_z)}{L(1+\phi_z)} \\ & & & \frac{EA}{L} & 0 & -\frac{\widehat{D}_{ab}}{L} \\ & & & & \frac{12\widehat{D}_b}{L^3(1+\phi_z)} & \frac{-6\widehat{D}_b}{L^2(1+\phi_z)} \\ & & & & & \frac{\widehat{D}_b(4+\phi_z)}{L(1+\phi_z)} \end{bmatrix} \quad (A8)$$

From the equilibrium equation, we deduce:

$$\theta_z(x) = \frac{\partial w}{\partial x} + c$$

Alternatively, c is integration constant of the equilibrium equation:

$$\frac{\partial^2\theta_z}{\partial x^2} = \frac{GAK_z c}{B\int E(z)z^2dz} = \frac{12c}{\phi_z L^2},\ \phi_z = \frac{12\int E(z)z^2dz}{L^2K_z\int G(z)dZ} \quad (A.9)$$

With $\phi_z = \frac{12BB}{L^2K_zD}$

ϕ_z is a coefficient which characterizes the transverse deformations. It depends on both the geometry and material characteristics of the section.